Molecular Tension Sensors Report Forces Generated by Single Integrin Molecules in Living Cells

Masatoshi Morimatsu, Armen H. Mekhdjian*, Arjun S. Adhikari, and Alexander R. Dunn*

Supporting Information

Materials and Methods

Cell Culture

Human foreskin fibroblast (HFF) cells CCD-1070Sk (ATCC CRL-2091) were cultured in DMEM high glucose medium (Gibco, Cat #21063-029) in the absence of phenol red and supplemented with 10% fetal bovine serum (FBS, Axenia Biologix), sodium pyruvate (1 mM, Gibco), MEM non-essential amino acids (1x, Gibco), and penicillin/streptomycin (100 U/mL and 100 µg/mL, Gibco). The cells were incubated at 37 °C with 5% CO_2. On the day of the experiment, cells were washed with phosphate-buffered saline (PBS) (Gibco), trypsinized using 0.25% Trypsin-EDTA (Gibco), seeded on functionalized coverslips in a custom-made chamber, and allowed to adhere for ~30 minutes. After this time the media was switched to Leibovitz's L15 medium (Gibco, Cat #21083-027) without phenol red to support cell growth in environments without CO_2 equilibration. All measurements were made within 1 hour of plating the cells. In single-molecule experiments, FBS was not added to the L15 medium due to high autofluorescence. Transient transfection of eGFP-tagged paxillin[1] was performing using Effectene Transfection Reagent (Qiagen) according to the manufacturer specifications.

Design of MTS and Expression

DNA encoding MTSs was synthesized by DNA 2.0 (Menlo Park, CA) for expression in *E. coli*. The full-length MTS consists of an N-terminal Flag-tag (DYKDDDDK) for purification, followed by an Avi-tag for biotinylation (GLNDIFEAQKIEWHE), lysine-cysteine (KC) for maleimide-labeling, 8 repeats of the GPGGA sequence, which acts as an entropic spring[2], an ACP tag domain for CoA labeling (BioLabs), the RGD peptide from fibronectin (TVYAVTGRGDSPASSAA), and a C-terminal 6x His-tag for purification. The full amino acid sequence is:

MDYKDDDDKGWGLNDIFEAQKIEWHEDVEAWLGARVPLVETKKCKEFGPGGAGPGGAGPGGAGPGGAGPGGAGP
GGAGPGGAGPGGAHMMSTIEERVKKIIGEQLGVKQEEVTNNASFVEDLGATSLGTVELVMALEEEFDTEIPDEEAEKIT
TVQAAIDYINGHQATVYAVTGRGDSPASSAAHHHHHH

The total size of this protein was calculated to be 19.546 kD from the amino acid sequence and confirmed by LC/MS on an Agilent 1260 HPLC and Bruker microTOF-Q II mass spectrometer to be 19.545 kD.

MTS Protein Expression and Purification

Plasmids were transformed into chemically competent BL21 DE3 *E. coli* cells. The cells were grown to an optical density of 0.6 at 37 °C in the presence of ampicillin, and induced by adding isopropyl β-D-1-thiogalactopyranoside (IPTG) to a final concentration of 0.238 mg/mL for 5 hours at 37 °C. The cells were harvested by centrifuging at 6000xG at 4 °C for 30 minutes. The cell pellet was resuspended in 50 mM sodium phosphate, 300 mM NaCl, 10 mM imidazole buffer (pH 8.0). 5 µM each of lysozyme, DNAse I, pepstatin A, leupeptin, and phenylmethylsulfonyl fluoride were added to the suspension and gently mixed at 4 °C for 45 minutes. The mixture was sonicated on ice for 5 cycles (30 seconds each), and then centrifuged at 14000xG at 4°C for 30 minutes. His PurNi-NTA Resin (ThermoScientific, Prod #88222) was added to the supernatant and gently mixed at 4 °C for 120 minutes. The protein was then purified using His-Tag affinity chromatography. Briefly, the supernatant with the nickel agarose beads was added to a 10 mL column, and the flow-through was collected. The resin was allowed to settle (avoiding drying out) and washed twice with 5 mL of buffer containing 50 mM sodium phosphate, 300 mM NaCl, 20 mM imidazole (pH 8.0). The protein was eluted with eight 500 µL aliquots of buffer containing 50 mM sodium phosphate, 300 mM sodium chloride, 250 mM imidazole (pH 8.0). All the samples were run on a denaturing polyacrylamide gel to determine which eluent fractions had the highest concentration of the desired product. Product-containing fractions were pooled and the concentration was determined using a UV-Vis spectrophotometer (NanoDrop, ThermoScientific). The MTS protein was flash frozen and stored at -80 °C.

Fluorescence labeling and biotinylaton of MTS

First, 100 µl of unlabeled MTS (~100 µM) was mixed with Alexa 546 maleimide (Life Technologies) at a molar ratio of 1:10 (protein:dye) and incubated for 30 min at 37 °C followed by overnight on ice. Afterwards, the sample was dialyzed using a Slide-A-Lyzer Dialysis Cassette Kit (10 kDa, Thermo Scientific) against 10 mM Tris-HCl buffer at pH 8.0 to remove unreacted Alexa 546 dyes. 40 µM MTS was biotinylated using BirA biotin ligase, Biomix-A, Biomix-B, and biotin (Avidity, LLC) according to the manufacturer specifications. The reaction was then extensively dialyzed against 20 mM HEPES (pH 7.0), and the biotinylation efficiency was confirmed by SDS PAGE (Figure S1). MTS labeled with both Alexa 546 and biotin was then diluted to a concentration of 10 µM in 50 mM HEPES, mixed with 1 mM DTT, 10 mM $MgCl_2$, 2 µM SFP synthase, and 50 µM CoA 647 Substrate (New England BioLabs Inc.), and incubated for 30 min at 37 °C followed by overnight on ice. Finally, fully-labeled MTS was dialyzed against 20 mM HEPES (pH 7.0) to remove unreacted CoA 647. The labeling efficiency of Alexa 546 and of CoA 647 was ~90% in both cases as quantified by UV-Vis absorption (NanoDrop).

Flow cell preparation

Custom-built imaging chambers were used for the single-molecule and ensemble measurements. Perfusion chambers (Grace Biolabs PC3L-1.0, Product #622103) were attached to biotinylated PEG-coated coverslips (MicroSurfaces, Inc). Neutravidin (2.0 mg/mL, Molecular Probes) was adsorbed on the

biotinylated PEG-coated coverslip. After washing by PBS, Pluronic F-127 (0.2% w/w) was added to prevent the non-specific attachment of sensors and cells. Fully-labeled MTS (~5-10 nM) and MTS lacking both fluorophores (~20 nM) for ensemble experiments, or fully-labeled MTS (~50-100 pM) and MTS lacking fluorophores (~100 nM) for single molecule experiments were then added to the flow cell and incubated for 10 min. After each addition step above, excess reagent was removed by washing with PBS. HFFs were then added, and incubated for 30 min at 37 °C in DMEM high glucose medium (see cell culture methods). Finally, the chamber was washed with serum-free L-15 supplemented with Trolox (2 mM), protocatechuic acid (PCA) (2.5 mM, Sigma-Aldrich), and protocatechuate-3,4-dioxygenase (PCD) (500 nM, Sigma-Aldrich) prior to measurement.[3]

Immunofluorescence Microscopy

Cells were fixed with a solution of 4% paraformaldehyde in PBS, permeabilized with a solution of 0.25% Triton X-100 in PBS and blocked with a solution of 1% BSA in PBS. Samples were then incubated with 1 µg/mL Hoechst 34580 (Life Technologies) in PBS for 10 minutes, followed by 10 µM TMR-phalloidin for 30 minutes, and finally with 10 µg/mL mouse anti-paxillin antibody (Millipore) and 10 µg/mL secondary goat anti-mouse IgG labeled with Alexa 647 (Life Technologies). The samples were imaged using an inverted Ti-Eclipse epifluorescent microscope (Nikon) with a 20x objective and sCMOS camera (Andor Neo) or an inverted laser scanning confocal microscope (Zeiss LSM 510 Meta) with a 20x or 40x objective. Image analysis was performed with ImageJ and Slidebook software.

Single molecule TIRF imaging

Single molecule fluorescence measurements were performed with objective-type total internal reflection fluorescence (TIRF) microscopy on an inverted microscope (Nikon TiE) with a Apo TIRF 100x oil objective lens (NA 1.49). Fluorescent dyes were excited with 532 nm (Crystalaser) and 635 nm (Blue Sky Research) lasers. Light emitted by Alexa 546 and CoA 647 were separated using custom-build optics. Key elements are a dual band dichroic filter with center/bandwidths of 580 nm/60 nm and 70 nm/100 nm, and a 675 nm/30 nm band-pass filter to reduce background in the acceptor channel. The channels were split and imaged on the same camera chip. Data were acquired at 4 frames per second with an EMCCD camera (iXon, Andor).

Single-molecule FRET calculations

Single molecule FRET calculations were done using custom-made MATLAB code. Donor and acceptor images are aligned and overlaid using a transformation vector determined using a calibration slide sparsely coated with multi-color 0.1 µm fluorescent beads (Molecular Probes, Life Technologies, Cat #T7279). The positions of individual molecules are determined manually based on acceptor intensities, or automatically using a custom-made spot-tracking algorithm in MATLAB (Tristan Ursell; Stanford University). Locating based on the acceptor intensities ensures the presence of an acceptor fluorophore on the molecule of interest. Mean fluorescence intensities are calculated for a 9x9 pixel area centered on the pixel with maximum intensity for each donor and acceptor. Acceptor and donor photobleaching events are identified manually. Donor and acceptor intensities are averaged over appropriate time

intervals to yield *A, A_b, D, D_b,* and *D_0 as* explained below (Figure S9). From those values we calculate the single molecule FRET efficiency E:

$$E = \frac{(A-A_b)}{(A-A_b)+\gamma\cdot(D-D_b)} \quad (1)$$

$$\gamma = \frac{(A-A_b)}{D_0-D} \quad (2)$$

or equivalently

$$E = \frac{(D_0-D)}{(D_0-D_b)} \quad (3)$$

A = acceptor intensity during FRET
A_b = background intensity in the acceptor channel
D = donor intensity during FRET
D_b = background intensity in the donor channel
D_0 = donor intensity after acceptor photobleaching
γ = correction factor accounting for relative dye quantum yields and detection efficiencies in the donor and acceptor channels

Established criteria were used to identify single molecule FRET events.[4] Single step photobleaching confirmed the presence of one donor and acceptor fluorophore. Only these spots were used for FRET calculations in our experiments. Control measurements indicate that changes in FRET signal are due to cell-generated forces: (i) probe recruitment to the coverslip surface only occurs if the probe is biotinylated and the surface is incubated with Neutravidin; ii) cells do not spread on the passivated surface in the absence of the MTS (Figure S2); iii) fluorescence signal is only present when the MTS is also present, and the number of fluorescent puncta scale with the amount of labeled MTS added to the flow chamber; iv) FRET values do not reflect spatial variations in illumination intensity; v) FRET values under zero load match the anticipated efficiency; vi) Changes in FRET depend on an intact cytoskeleton (Figure S8); vii) Probes designed to be insensitive to applied tension do not show FRET changes in the presence of cells (Figures S6, S7, S11, S12)

To investigate the possible presence of MTS molecules under sufficient tension to cause 0% FRET, we first identified FRET donor and acceptor fluorophores that colocalized with direct excitation by 532 nm and 635 nm lasers, but that exhibited ~0% FRET. Using these criteria, we analyzed 563 colocalized molecules in the presence of cells and observed undetectably low FRET in 7% of these molecules. Of these low FRET events, about 75% were underneath the cell, while the remaining 25% were located in the same field of view but outside the cell periphery. On average, 60% of the field of view lay inside the cell periphery. In short, we observe that only a small portion (7%) of the MTS molecules exhibit ~0% FRET, and moreover that these molecules are comparably likely both inside and outside the cell periphery. These factors suggest that many of the 0% FRET observations do not reflect > 6 pN forces exerted on the MTS, but instead reflect some process that is rare and independent of the presence of

cells. It is possible that in these instances the acceptor fluorophore photobleaches immediately prior to excitation by the 532 nm laser, or that two separate, singly-labeled molecules colocalize to the same analysis region.

Ensemble FRET calculations (FRET Index)

Ensemble FRET is reported as a FRET index as opposed to an absolute FRET efficiency as in the single-molecule case due to the presence of some singly-labeled sensors, which causes the FRET value to be slightly lower than the absolute FRET efficiency. To calculate FRET index, we divide the acceptor intensity (background subtracted) by the sum of the acceptor and donor intensities (also background subtracted). This calculation assumes that the correction factor γ is 1.[3] This assumption is in good agreement with our single molecule measurements, which yield a median value for γ of 1.1.

FRET efficiency to force calculation

The $(GPGGA)_8$ protein spring domain and FRET pair used in the present study are highly similar to the Cy3/Cy5 FRET pair and spring domain, termed TSModCy, used in the original calibration of TSMod.[2] The single-molecule calibration performed by Grashoff *et al.* thus provides a means of relating measured FRET to tensions at the molecular level.[2] We extracted the data points from the published force vs. FRET curve for TSModCy, neglecting all negative values for the FRET efficiency. We converted these FRET values to distances using an R_0 of ~6.0 nm for Cy3 and Cy5.[2] This yields a force-extension curve $R(f)$ for the $(GPGGA)_8$ domain.

The measured no-load FRET efficiency for the MTS used in our study is 47%. Using a Förster radius of 6.5 nm for Alexa 546 and Alexa 647,[5, 6] we calculated the no-load donor-acceptor distance D_{MTS} to be 6.65 nm. The resting length of TSModCy $D_{TSModCy}$ is 6.0 nm based on the no-load FRET efficiency of ~50%. Following Grashoff *et al.*, we model the force-dependent donor-acceptor distance in the MTS as:

$$R = D_{MTS} - D_{TSModCy} + R(f) \qquad (4)$$

Where the donor-acceptor distance R incorporates the difference in resting lengths of MTS and TSModCy (D_{MTS}-$D_{TSModCy}$) plus the force dependent increase in length $R(f)$. The distance vs. force curve for MTS was then converted to FRET vs. force using the standard FRET equation and the R_0 of our dyes.

$$E = \left[1 + \left(\frac{R}{R_0}\right)^6\right]^{-1} \qquad (5)$$

We then fit the resultant data points to a 4th-order polynomial to provide a phenomenological relation between FRET and force. Errors in R_0 do not have a strong influence on calculated forces: Figure S13 shows several calibration curves calculated using R_0 values ranging from 5.0 nm to 8.0 nm.

References

(1) Laukaitis, C. M.; Webb, D. J.; Donais, K.; Horwitz, A. F. *J. Cell Biol.* **2001,** *153* (7), 1427-1440.

(2) Grashoff, C.; Hoffman, B. D.; Brenner, M. D.; Zhou, R.; Parsons, M.; Yang, M. T.; McLean, M. A.; Sligar, S. G.; Chen, C. S.; Ha, T.; Schwartz, M. A. *Nature* **2010**, *466* (7303), 263-266.

(3) Aitken, C. E.; Marshall, R. A.; Puglisi, J. D. *Biophys. J.* **2008**, *94* (5), 1826-1835.

(4) Roy, R.; Hohng, S.; Ha, T. *Nat. Methods* **2008**, *5* (6), 507-516.

(5) Huang, F.; Rajagopalan, S.; Settanni, G.; Marsh, R. J.; Armoogum, D. A.; Nicolaou, N.; Bain A. J.; Lerner, E.; Haas, E.; Ying, L.; Fersht, A. R. *Proc. Natl. Acad. Sci. U. S. A.* **2009**, *106* (49), 20758-20763.

(6) Kuzmenkina, E. V.; Heyes, C. D.; Nienhaus, G. U. *Proc. Natl. Acad. Sci. U. S. A.* **2005**, *102* (43), 15471-15476.

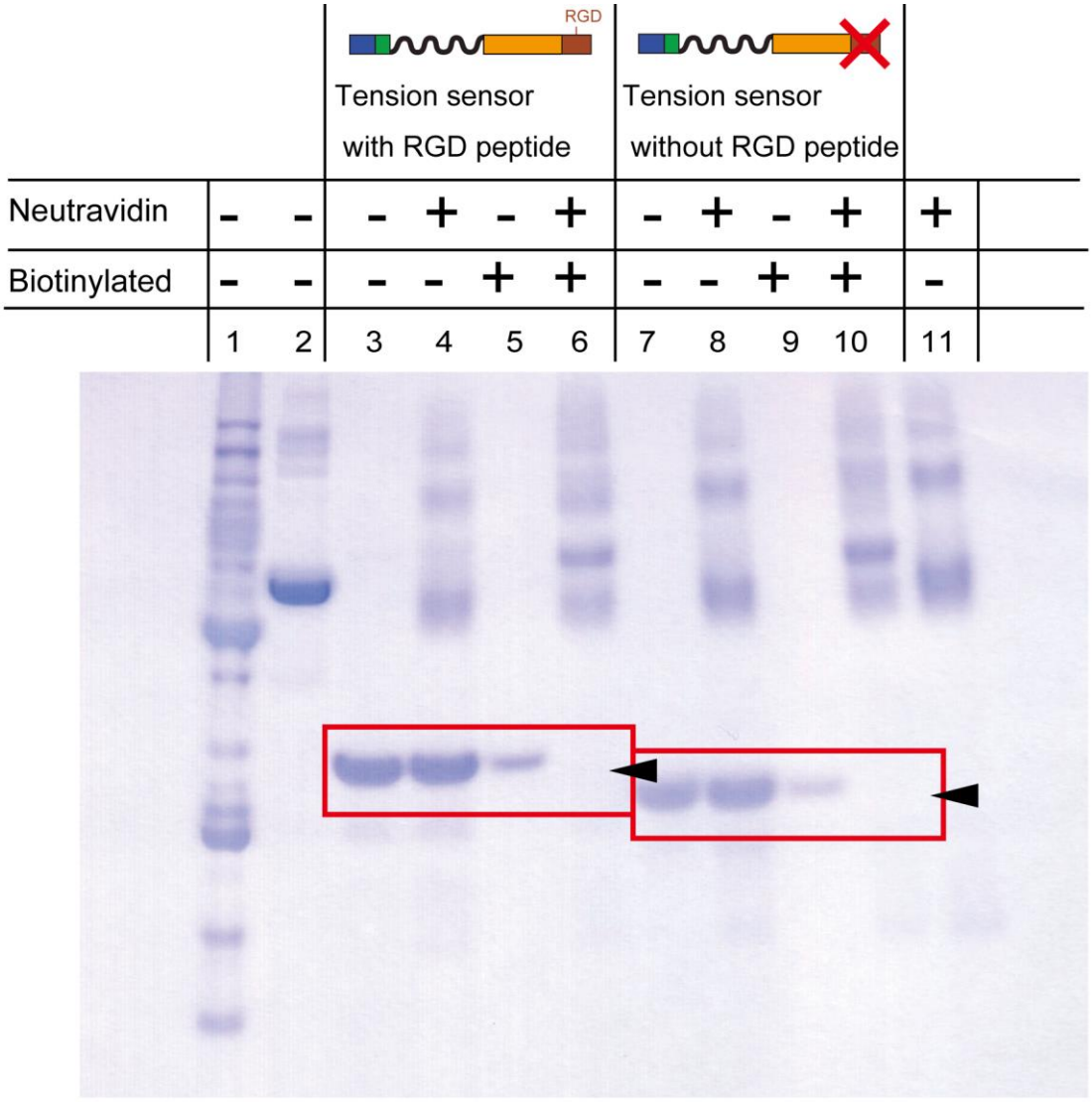

Supplementary Figure 1. SDS PAGE gel characterizing the biotinylation of MTS. From left to right, 1. Benchmark™ protein ladder, 2. BSA, 3. MTS, 4. Non-biotinylated MTS plus Neutravidin, 5. Biotinylated MTS, 6. Biotinylated MTS plus Neutravidin, 7. MTS lacking RGD sequence (noRGD MTS), 8. Non-biotinylated noRGD MTS plus Neutravidin, 9. Biotinylated noRGD MTS, 10. Biotinylated noRGD MTS plus Neutravidin, 11. Neutravidin. Biotinylated MTS and noRGD MTS bind to Neutravidin, forming a complex that runs at higher molecular weight than the uncomplexed sensor. Neutravidin runs as a series of bands between 50 and *ca.* 100 kDa, reflecting partial dissociation of the Neutravidin tetramer. The black arrows indicate the absence of a band when the biotinylated MTS is incubated with Neutravidin, demonstrating efficient binding.

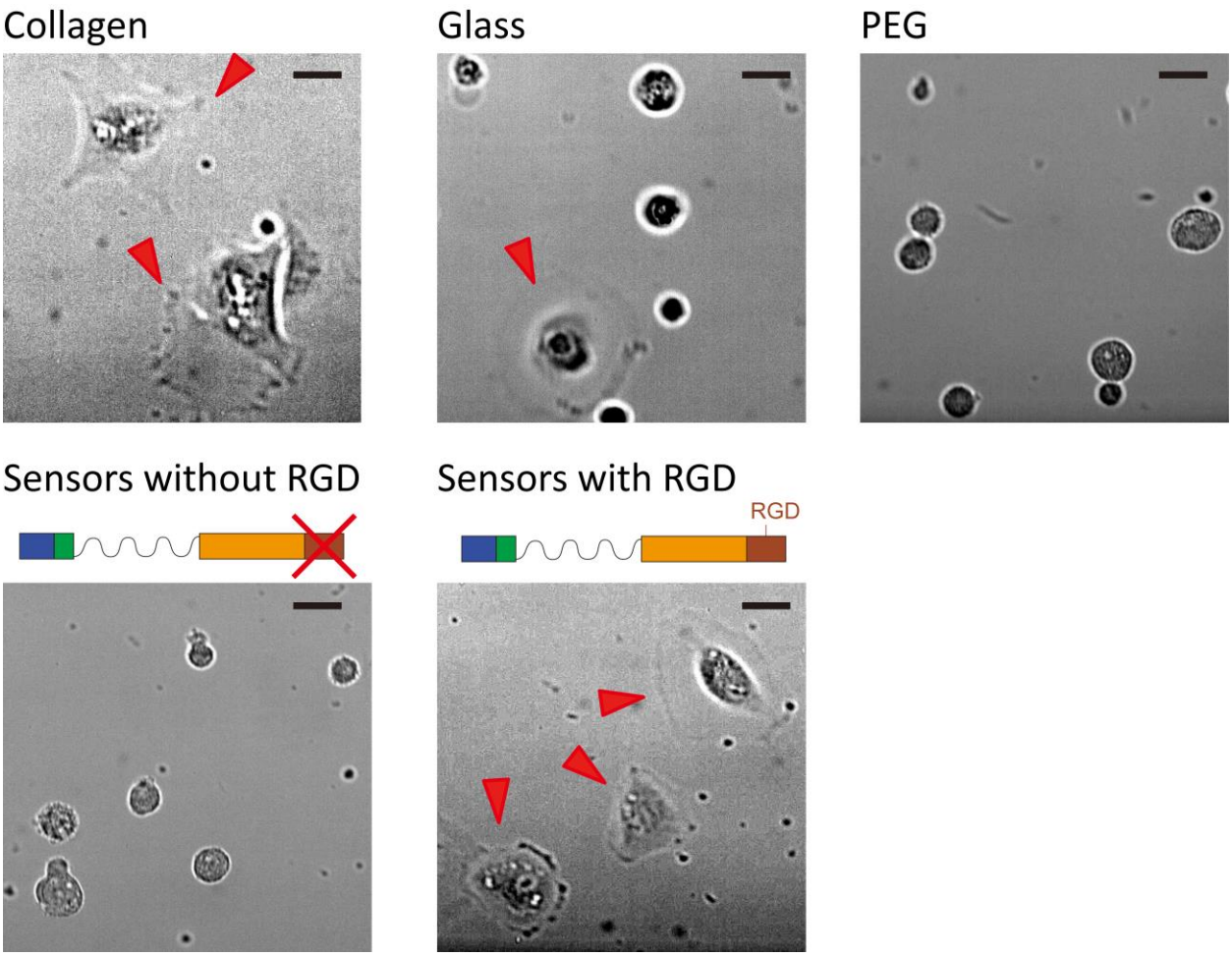

Supplementary Figure 2. Brightfield images of HFFs on various functionalized surfaces after 60 min incubation. HFFs spread well on surfaces coated with collagen or the MTS, but do not spread on PEG passivated coverslips or on coverslips functionalized with MTS probes lacking the RGD sequence. Red arrows indicate spread cells. Scale bar in all images is 30 µm.

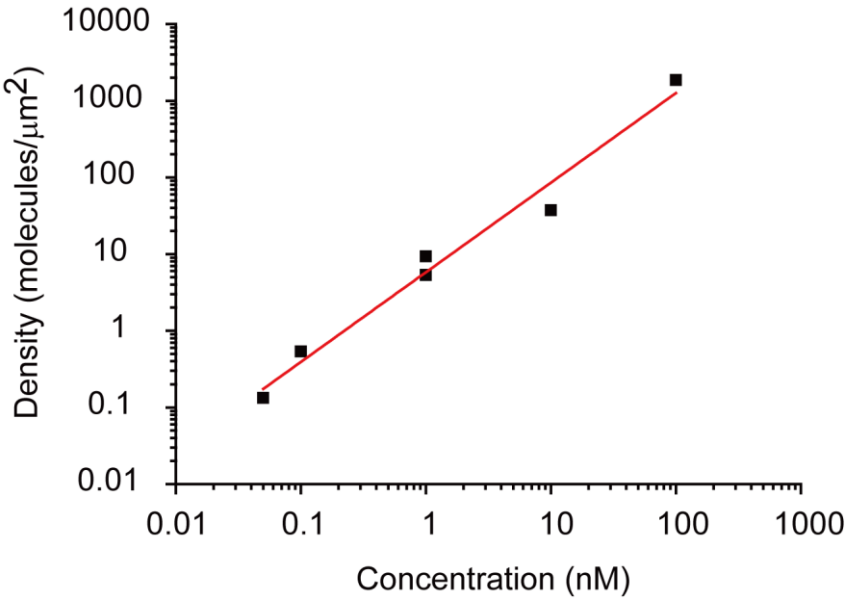

Supplementary Figure 3. Determination of MTS surface density as a function of MTS concentration added during flow cell preparation. Densities below 1 molecule per μm^2 were determined by exciting at 635 nm and then counting the number of immobilized fluorophores per field of view, yielding 50 and 200 molecules per 375 μm^2 for the 0.05 nM and 0.1 nM concentrations, respectively. The density at 1 nM was determined by quantifying the background-subtracted mean intensity in a field of view, and then comparing this value to the background-subtracted mean intensity at 0.05 nM and 0.1 nM added MTS. The gain and exposure of the camera were maintained when comparing these intensities. This procedure allows us to compare single molecule and ensemble fluorophore density measurements. The gain and exposure settings were then decreased to allow for greater dynamic range, and the background-subtracted intensities were determined for 1, 10, and 100 nM added MTS. We observed a linear increase in fluorescence intensity with increasing probe concentration, allowing us to extrapolate the surface density of molecules at 10 and 100 nM added MTS.

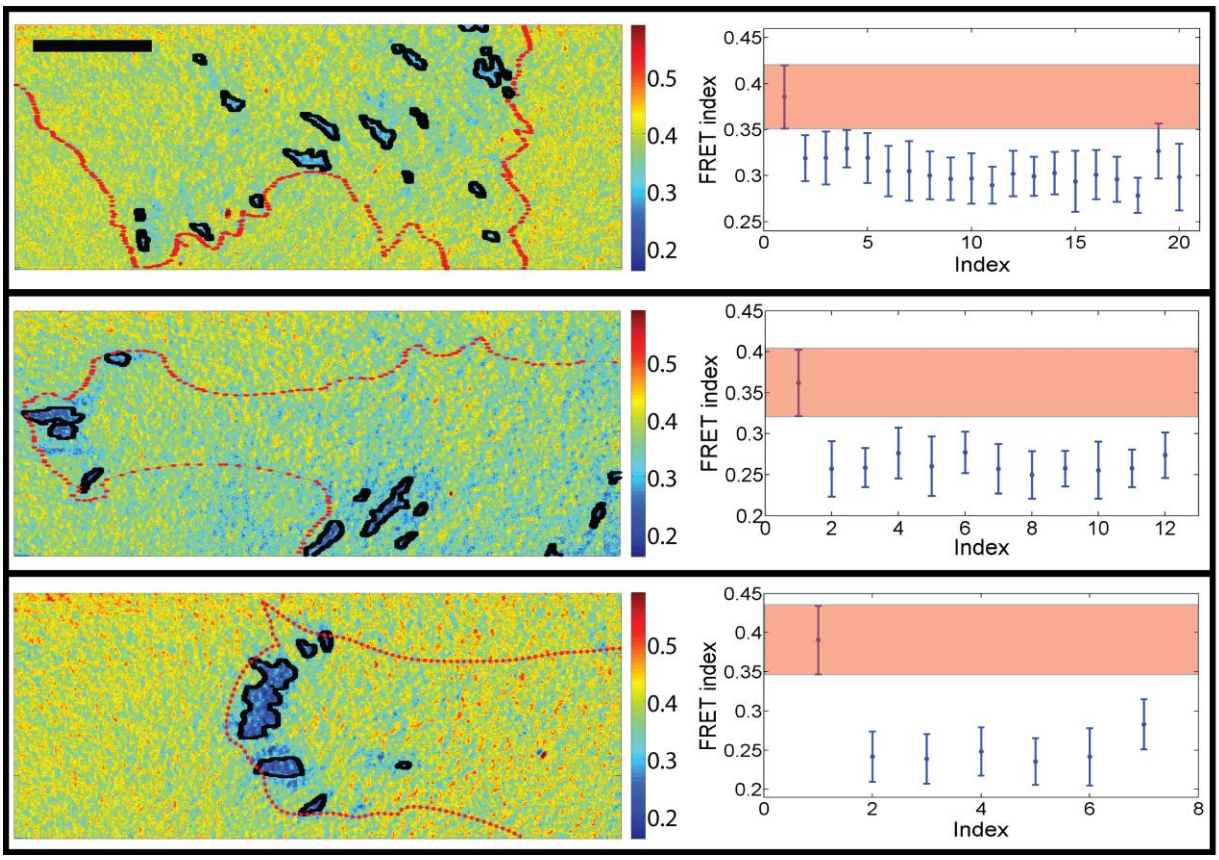

Supplementary Figure 4. Example cells displaying low FRET regions (outlined in black). The cell outline is shown in red (from corresponding brightfield images). The plots show the average FRET index in the outlined regions, with the x-axis indices corresponding to each of the regions from left to right. Note that index "1" refers to the average of all the pixels not enclosed by the black outline. The pink bar represents the 95% confidence interval for the FRET values in the regions not encompassed by the black outlines. The error bars represent the standard deviations of the FRET index calculated for all the outlined regions. Scale bar in all images is 10 µm.

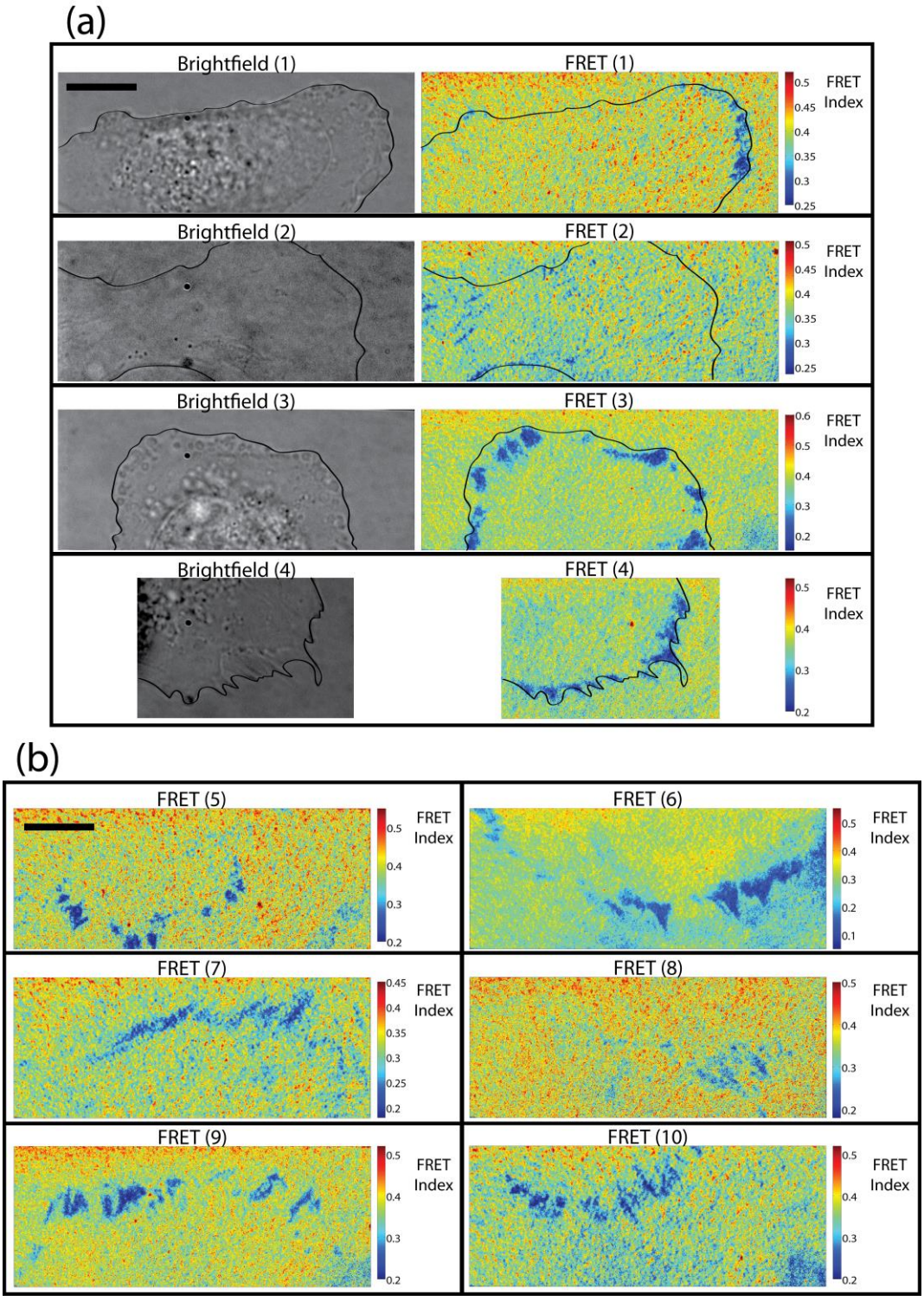

Supplementary Figure 5. a) HFF cells show distinct low FRET regions at the cell periphery. b) Six additional FRET maps for example cells. Low FRET regions mimic patterns of focal adhesions. Scale bar in all images is 10 µm.

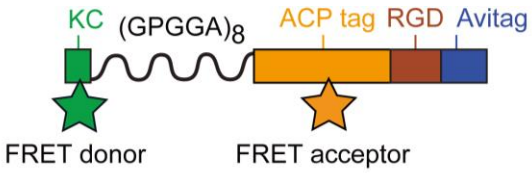

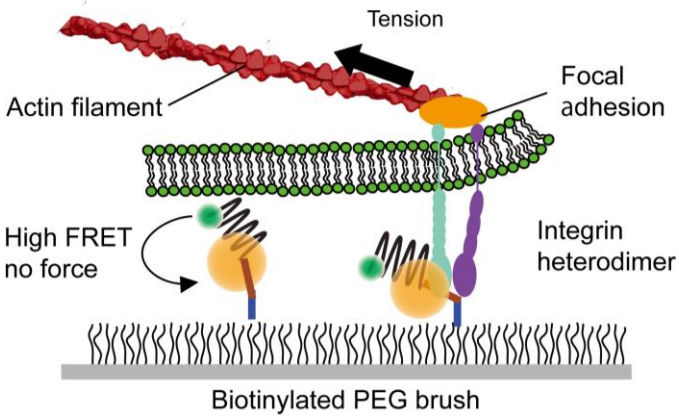

Supplemental Figure 6. Schematic diagram for the flipped MTS. The Avitag biotinylation site (blue) is located C-terminal to the RGD domain (brown), and preceding the terminal His-tag. When cells are plated on these sensors the integrins interact with the RGD domain and force propagates to the glass coverslip without stretching the fluorophore-flanked $(GPGGA)_8$ spring.

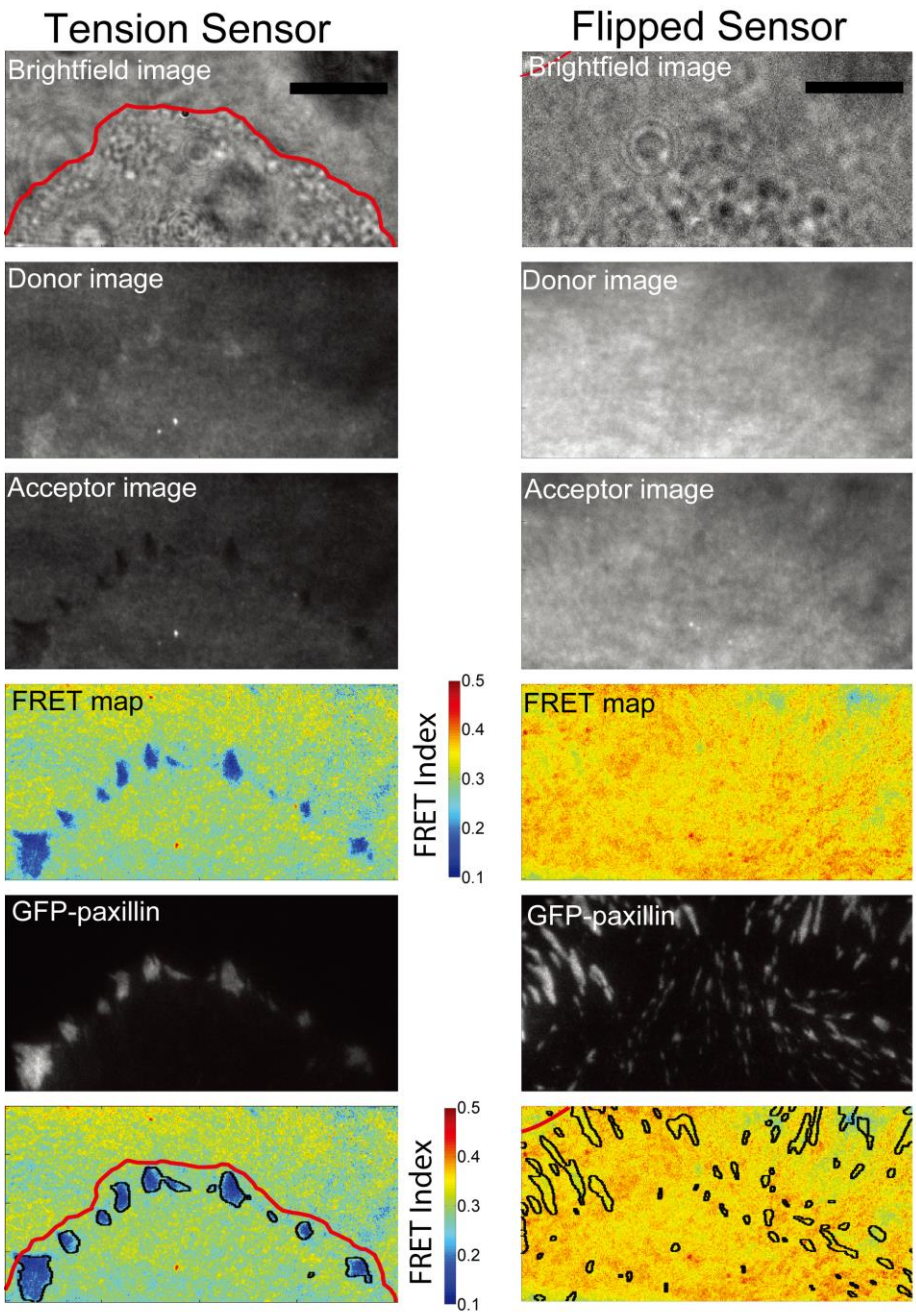

Supplemental Figure 7. *Top row:* Brightfield images of cells plated atop the MTS or flipped sensor (see Figure S6). *2nd, 3rd rows*: Donor and acceptor channels show colocalized increased donor and decreased acceptor fluorescence, indicative of decreased FRET. *4th row*: FRET maps. *5th row*: eGFP-paxillin, showing the presence of robust FAs. 6th row: cell periphery and FAs outlined in *red* and *black*. Note large localized decreases in FRET for the MTS but not for the flipped sensor. Scale bar in all images is 10 µm.

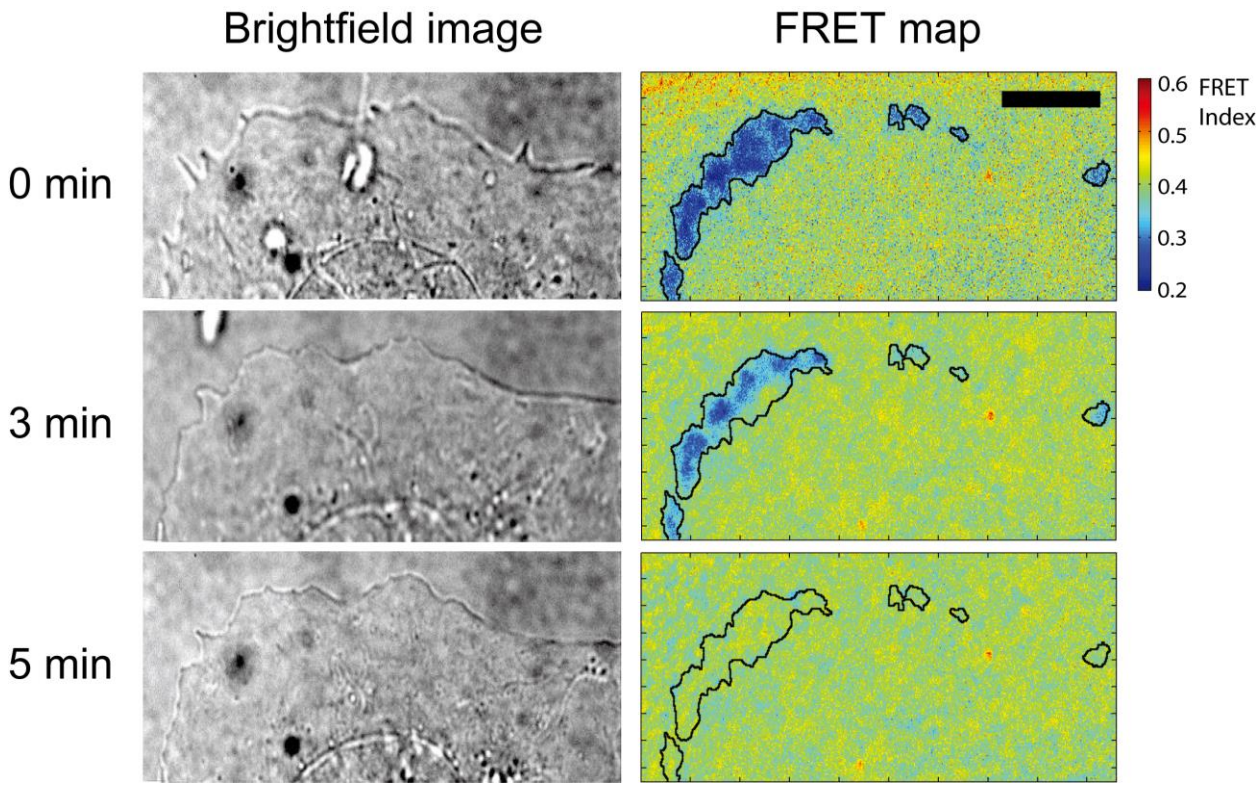

Supplemental Figure 8. Addition of 1 µM cytochalasin D, an actin depolymerizing agent, disrupts force at integrin complexes within 5 minutes. The black outline traces the low FRET regions prior to the addition of cytochalasin D. Scale bar in all images is 10 µm.

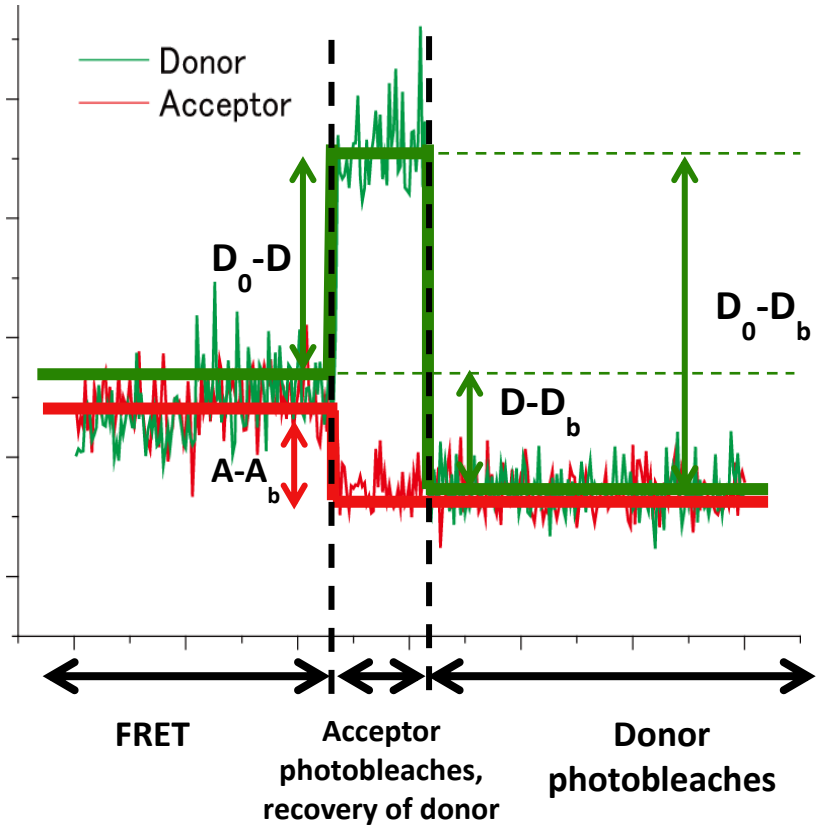

Supplementary Figure 9. Single-molecule trace exhibiting two-step photobleaching. The observation of sequential acceptor and donor photobleaching events confirms the presence of 1 donor and 1 acceptor fluorophore on the molecule of interest. FRET efficiency *E* can be calculated using $= \frac{(A-A_b)}{(A-A_b)+\gamma\cdot(D-D_b)}$. The variable $\gamma = (A\text{-}A_b)/(D_0\text{-}D)$, reflecting the relative quantum yields and photon collection efficiencies for the two fluorophores. FRET efficiency can also be calculated as $= \frac{D_0-D}{D_0-D_b}$. These treatments are mathematically equivalent at the single-molecule level.

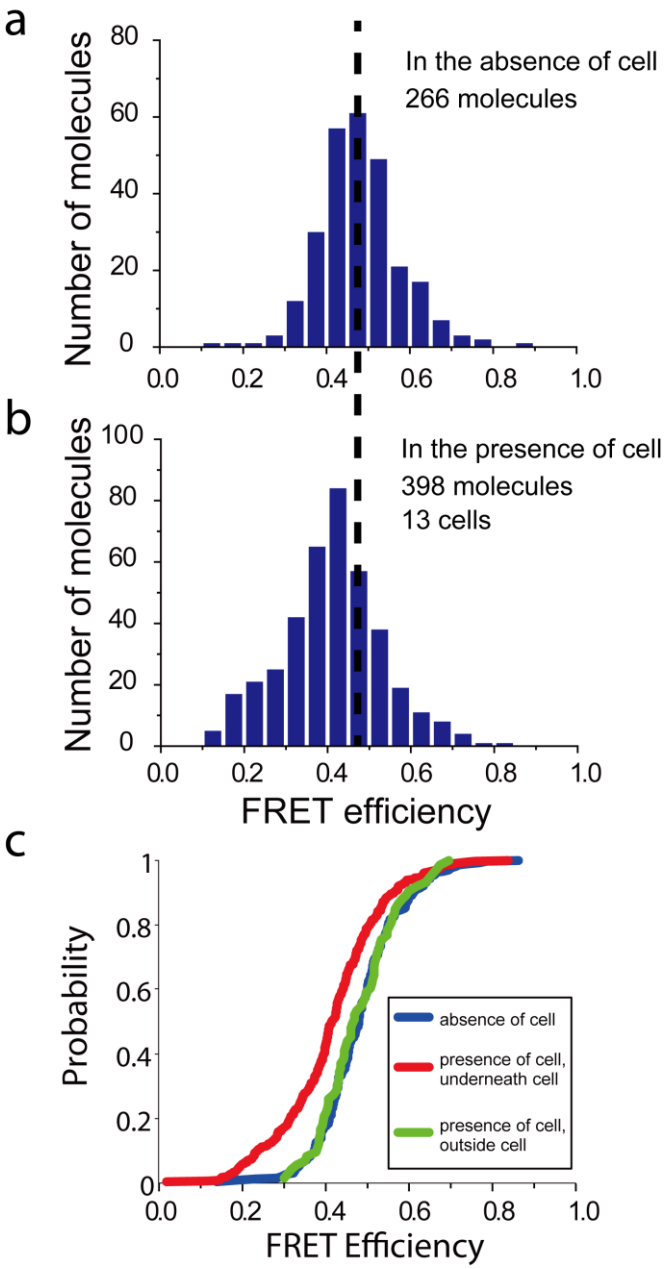

Supplementary Figure 10. FRET efficiency distributions in the (a) absence of cells and (b) presence of cells. These distributions are statistically different as quantified by the two-sample Kolmogorov-Smirnov test (p-value: 1.7×10^{-12}). (c) Molecules analyzed in the presence of cells but not underneath a cell (green; 73 molecules, 5 cells) reproduce the FRET efficiency distribution recorded in the absence of cells (blue; 266 molecules). These distributions are statistically the same with a p-value of 0.88. Both differ from the distribution of FRET values for molecules in the presence of cells and inside the cell periphery (red; 398 molecules, 13 cells).

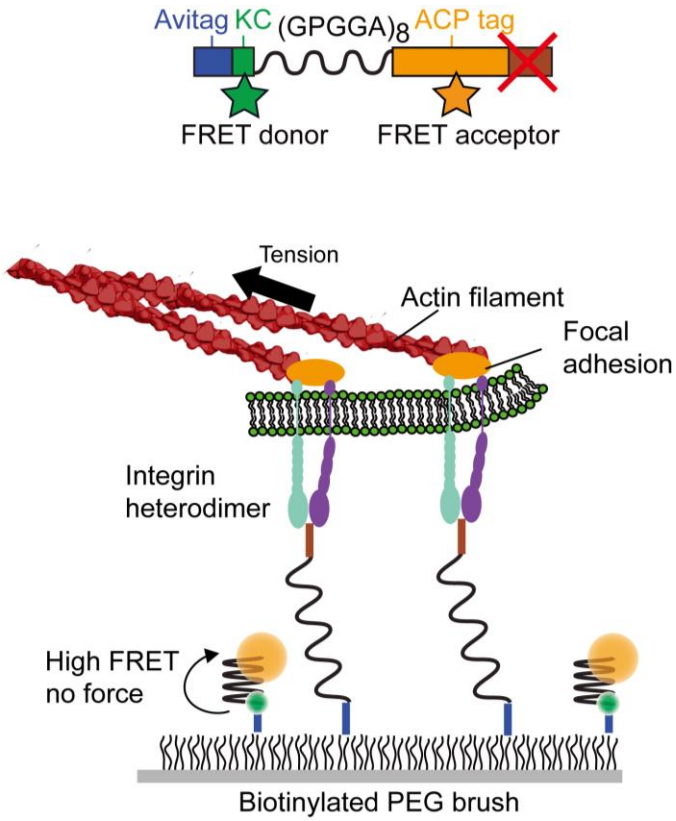

Supplementary Figure 11. Schematic diagram for the noRGD MTS experiment. Full-length MTSs lacking fluorophores are added at the density necessary for cell adhesion. Fluorophore-labeled MTSs lacking the RGD domain (noRGD MTS) are included at the low density necessary for single-molecule analysis. Thus, cells spread robustly on the surface but the fluorophore-labeled probes cannot interact with integrins.

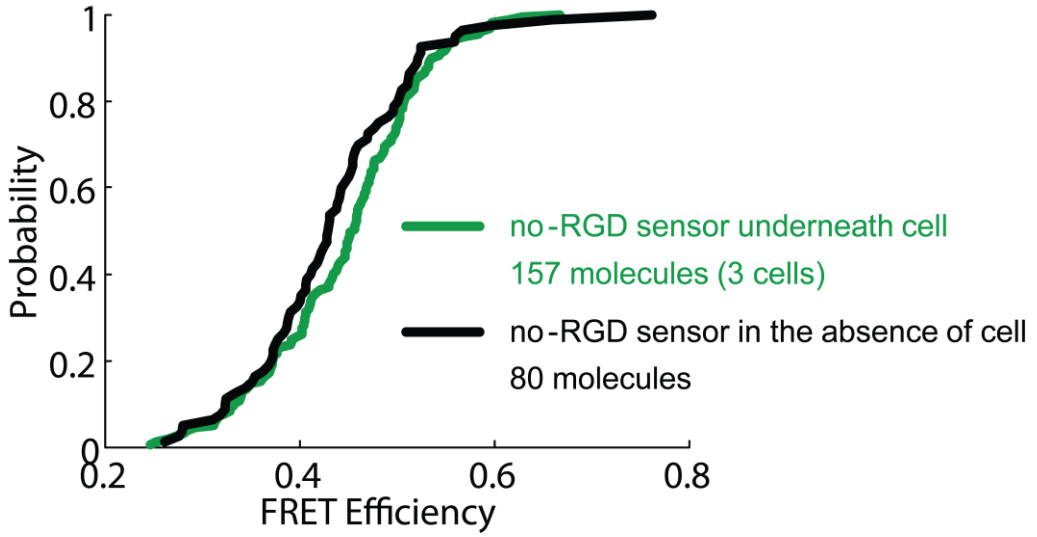

Supplementary Figure 12. Cumulative distributions for noRGD MTS in the absence (black; 80 molecules) and presence of cells (green; 157 molecules, 3 cells). These distributions are not statistically distinguishable (p-value of 0.06 by the two-sample Kolmogorov-Smirnov test).

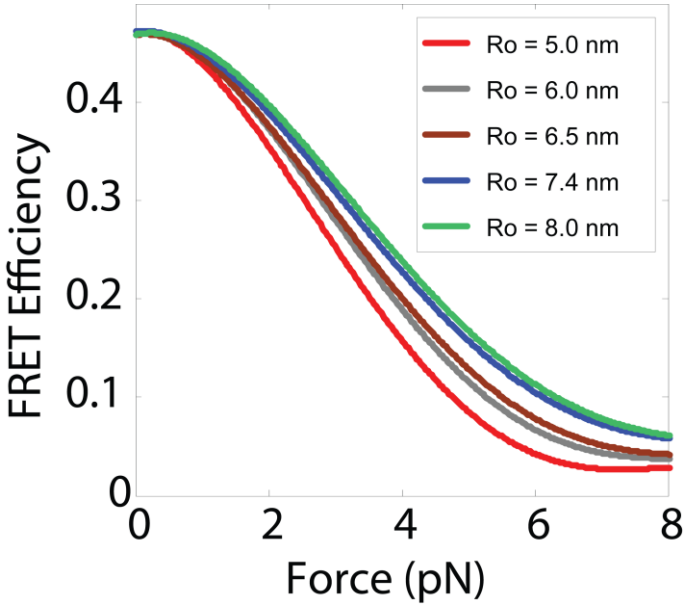

Supplementary Figure 13. FRET versus force calibration curves calculated with Förster radii ranging from 5.0 to 8.0 nm show that even large errors in R_0 lead to modest, single-pN changes in the calculated force.

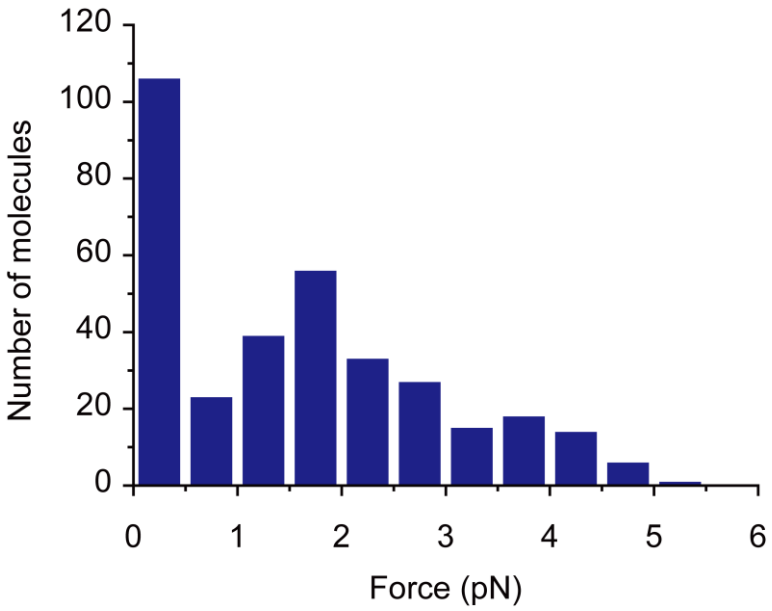

Supplementary Figure 14. Force distribution for MTS molecules underneath the cell indicates that a population of molecules experiences tensions in the 1-5 pN range. Forces are calculated using the FRET-force calibration curve shown in Figure S13 with an R_0 of 6.5 nm. FRET efficiencies greater than 47% are counted as being under no force (0 pN).

Supplementary Movie 1. Raw experimental data and corresponding FRET index map. The three channels from top to bottom are donor intensity, acceptor intensity, and FRET index. In this movie we move the stage to image most of the cell area, which is larger than the field of view. Note the low acceptor fluorescence and high donor fluorescence in regions of low FRET, indicative of donor de-quenching.